Search for Universal Extra Dimensions in $p\bar{p}$ Collisions

V. M. Abazov,[34] B. Abbott,[72] B. S. Acharya,[28] M. Adams,[48] T. Adams,[46] G. D. Alexeev,[34] G. Alkhazov,[38] A. Alton,[60,†] G. Alverson,[59] M. Aoki,[47] A. Askew,[46] B. Åsman,[40] S. Atkins,[57] O. Atramentov,[64] K. Augsten,[9] C. Avila,[7] J. BackusMayes,[79] F. Badaud,[12] L. Bagby,[47] B. Baldin,[47] D. V. Bandurin,[46] S. Banerjee,[28] E. Barberis,[59] P. Baringer,[55] J. Barreto,[3] J. F. Bartlett,[47] U. Bassler,[17] V. Bazterra,[48] A. Bean,[55] M. Begalli,[3] C. Belanger-Champagne,[40] L. Bellantoni,[47] S. B. Beri,[26] G. Bernardi,[16] R. Bernhard,[21] I. Bertram,[41] M. Besançon,[17] R. Beuselinck,[42] V. A. Bezzubov,[37] P. C. Bhat,[47] S. Bhatia,[62] V. Bhatnagar,[26] G. Blazey,[49] S. Blessing,[46] K. Bloom,[63] A. Boehnlein,[47] D. Boline,[69] E. E. Boos,[36] G. Borissov,[41] T. Bose,[58] A. Brandt,[75] O. Brandt,[22] R. Brock,[61] G. Brooijmans,[67] A. Bross,[47] D. Brown,[16] J. Brown,[16] X. B. Bu,[47] M. Buehler,[47] V. Buescher,[23] V. Bunichev,[36] S. Burdin,[41,‡] T. H. Burnett,[79] C. P. Buszello,[40] B. Calpas,[14] E. Camacho-Pérez,[31] M. A. Carrasco-Lizarraga,[55] B. C. K. Casey,[47] H. Castilla-Valdez,[31] S. Chakrabarti,[69] D. Chakraborty,[49] K. M. Chan,[53] A. Chandra,[77] E. Chapon,[17] G. Chen,[55] S. Chevalier-Théry,[17] D. K. Cho,[74] S. W. Cho,[30] S. Choi,[30] B. Choudhary,[27] S. Cihangir,[47] D. Claes,[63] J. Clutter,[55] M. Cooke,[47] W. E. Cooper,[47] M. Corcoran,[77] F. Couderc,[17] M.-C. Cousinou,[14] A. Croc,[17] D. Cutts,[74] A. Das,[44] G. Davies,[42] S. J. de Jong,[33] E. De La Cruz-Burelo,[31] F. Déliot,[17] R. Demina,[68] D. Denisov,[47] S. P. Denisov,[37] S. Desai,[47] C. Deterre,[17] K. DeVaughan,[63] H. T. Diehl,[47] M. Diesburg,[47] P. F. Ding,[43] A. Dominguez,[63] T. Dorland,[79] A. Dubey,[27] L. V. Dudko,[36] D. Duggan,[64] A. Duperrin,[14] S. Dutt,[26] A. Dyshkant,[49] M. Eads,[63] D. Edmunds,[61] J. Ellison,[45] V. D. Elvira,[47] Y. Enari,[16] H. Evans,[51] A. Evdokimov,[70] V. N. Evdokimov,[37] G. Facini,[59] T. Ferbel,[68] F. Fiedler,[23] F. Filthaut,[33] W. Fisher,[61] H. E. Fisk,[47] M. Fortner,[49] H. Fox,[41] S. Fuess,[47] A. Garcia-Bellido,[68] G. A. García-Guerra,[31,§] V. Gavrilov,[35] P. Gay,[12] W. Geng,[14,61] D. Gerbaudo,[65] C. E. Gerber,[48] Y. Gershtein,[64] G. Ginther,[47,68] G. Golovanov,[34] V. N. Goryachev,[37] A. Goussiou,[79] P. D. Grannis,[69] S. Greder,[18] H. Greenlee,[47] Z. D. Greenwood,[57] E. M. Gregores,[4] G. Grenier,[19] Ph. Gris,[12] J.-F. Grivaz,[15] A. Grohsjean,[17,‖] S. Grünendahl,[47] M. W. Grünewald,[29] T. Guillemin,[15] G. Gutierrez,[47] P. Gutierrez,[72] A. Haas,[67,¶] S. Hagopian,[46] J. Haley,[59] L. Han,[6] K. Harder,[43] A. Harel,[68] J. M. Hauptman,[54] J. Hays,[42] T. Head,[43] T. Hebbeker,[20] D. Hedin,[49] H. Hegab,[73] A. P. Heinson,[45] U. Heintz,[74] C. Hensel,[22] I. Heredia-De La Cruz,[31] K. Herner,[60] G. Hesketh,[43,**] M. D. Hildreth,[53] R. Hirosky,[78] T. Hoang,[46] J. D. Hobbs,[69] B. Hoeneisen,[11] M. Hohlfeld,[23] Z. Hubacek,[9,17] V. Hynek,[9] I. Iashvili,[66] Y. Ilchenko,[76] R. Illingworth,[47] A. S. Ito,[47] S. Jabeen,[74] M. Jaffré,[15] D. Jamin,[14] A. Jayasinghe,[72] R. Jesik,[42] K. Johns,[44] M. Johnson,[47] A. Jonckheere,[47] P. Jonsson,[42] J. Joshi,[26] A. W. Jung,[47] A. Juste,[39] K. Kaadze,[56] E. Kajfasz,[14] D. Karmanov,[36] P. A. Kasper,[47] I. Katsanos,[63] R. Kehoe,[76] S. Kermiche,[14] N. Khalatyan,[47] A. Khanov,[73] A. Kharchilava,[66] Y. N. Kharzheev,[34] J. M. Kohli,[26] A. V. Kozelov,[37] J. Kraus,[61] S. Kulikov,[37] A. Kumar,[66] A. Kupco,[10] T. Kurča,[19] V. A. Kuzmin,[36] S. Lammers,[51] G. Landsberg,[74] P. Lebrun,[19] H. S. Lee,[30] S. W. Lee,[54] W. M. Lee,[47] J. Lellouch,[16] H. Li,[13] L. Li,[45] Q. Z. Li,[47] S. M. Lietti,[5] J. K. Lim,[30] D. Lincoln,[47] J. Linnemann,[61] V. V. Lipaev,[37] R. Lipton,[47] Y. Liu,[6] A. Lobodenko,[38] M. Lokajicek,[10] R. Lopes de Sa,[69] H. J. Lubatti,[79] R. Luna-Garcia,[31,††] A. L. Lyon,[47] A. K. A. Maciel,[2] D. Mackin,[77] R. Madar,[17] R. Magaña-Villalba,[31] S. Malik,[63] V. L. Malyshev,[34] J. Mansour,[22] Y. Maravin,[56] J. Martínez-Ortega,[31] R. McCarthy,[69] C. L. McGivern,[55] M. M. Meijer,[33] A. Melnitchouk,[62] D. Menezes,[49] P. G. Mercadante,[4] M. Merkin,[36] A. Meyer,[20] J. Meyer,[22] F. Miconi,[18] N. K. Mondal,[28] G. S. Muanza,[14] M. Mulhearn,[78] E. Nagy,[14] M. Naimuddin,[27] M. Narain,[74] R. Nayyar,[27] H. A. Neal,[60] J. P. Negret,[7] P. Neustroev,[38] S. F. Novaes,[5] T. Nunnemann,[24] G. Obrant,[38,*] J. Orduna,[77] N. Osman,[14] J. Osta,[53] G. J. Otero y Garzón,[1] M. Padilla,[45] A. Pal,[75] N. Parashar,[52] V. Parihar,[74] S. K. Park,[30] R. Partridge,[74,¶] N. Parua,[51] A. Patwa,[70] B. Penning,[47] M. Perfilov,[36] Y. Peters,[43] K. Petridis,[43] G. Petrillo,[68] P. Pétroff,[15] R. Piegaia,[1] M.-A. Pleier,[70] P. L. M. Podesta-Lerma,[31,‡‡] V. M. Podstavkov,[47] P. Polozov,[35] A. V. Popov,[37] M. Prewitt,[77] D. Price,[51] N. Prokopenko,[37] J. Qian,[60] A. Quadt,[22] B. Quinn,[62] M. S. Rangel,[2] K. Ranjan,[27] P. N. Ratoff,[41] I. Razumov,[37] P. Renkel,[76] M. Rijssenbeek,[69] I. Ripp-Baudot,[18] F. Rizatdinova,[73] M. Rominsky,[47] A. Ross,[41] C. Royon,[17] P. Rubinov,[47] R. Ruchti,[53] G. Safronov,[35] G. Sajot,[13] P. Salcido,[49] A. Sánchez-Hernández,[31] M. P. Sanders,[24] B. Sanghi,[47] A. S. Santos,[5] G. Savage,[47] L. Sawyer,[57] T. Scanlon,[42] R. D. Schamberger,[69] Y. Scheglov,[38] H. Schellman,[50] T. Schliephake,[25] S. Schlobohm,[79] C. Schwanenberger,[43] R. Schwienhorst,[61] J. Sekaric,[55] H. Severini,[72] E. Shabalina,[22] V. Shary,[17] A. A. Shchukin,[37] R. K. Shivpuri,[27] V. Simak,[9] V. Sirotenko,[47] P. Skubic,[72] P. Slattery,[68] D. Smirnov,[53] K. J. Smith,[66] G. R. Snow,[63] J. Snow,[71] S. Snyder,[70] S. Söldner-Rembold,[43] L. Sonnenschein,[20] K. Soustruznik,[8] J. Stark,[13] V. Stolin,[35] D. A. Stoyanova,[37] M. Strauss,[72] D. Strom,[48] L. Stutte,[47] L. Suter,[43] P. Svoisky,[72] M. Takahashi,[43] A. Tanasijczuk,[1] M. Titov,[17] V. V. Tokmenin,[34] Y.-T. Tsai,[68] K. Tschann-Grimm,[69] D. Tsybychev,[69] B. Tuchming,[17] C. Tully,[65] L. Uvarov,[38] S. Uvarov,[38] S. Uzunyan,[49] R. Van Kooten,[51] W. M. van Leeuwen,[32] N. Varelas,[48] E. W. Varnes,[44] I. A. Vasilyev,[37] P. Verdier,[19] L. S. Vertogradov,[34]

M. Verzocchi,[47] M. Vesterinen,[43] D. Vilanova,[17] P. Vokac,[9] H. D. Wahl,[46] M. H. L. S. Wang,[47] J. Warchol,[53] G. Watts,[79]
M. Wayne,[53] M. Weber,[47,§§] J. Weichert,[23] L. Welty-Rieger,[50] A. White,[75] D. Wicke,[25] M. R. J. Williams,[41]
G. W. Wilson,[55] M. Wobisch,[57] D. R. Wood,[59] T. R. Wyatt,[43] Y. Xie,[47] R. Yamada,[47] W.-C. Yang,[43] T. Yasuda,[47]
Y. A. Yatsunenko,[34] W. Ye,[69] Z. Ye,[47] H. Yin,[47] K. Yip,[70] S. W. Youn,[47] T. Zhao,[79] B. Zhou,[60] J. Zhu,[60] M. Zielinski,[68]
D. Zieminska,[51] and L. Zivkovic[74]

(The D0 Collaboration)

[1]*Universidad de Buenos Aires, Buenos Aires, Argentina*
[2]*LAFEX, Centro Brasileiro de Pesquisas Físicas, Rio de Janeiro, Brazil*
[3]*Universidade do Estado do Rio de Janeiro, Rio de Janeiro, Brazil*
[4]*Universidade Federal do ABC, Santo André, Brazil*
[5]*Instituto de Física Teórica, Universidade Estadual Paulista, São Paulo, Brazil*
[6]*University of Science and Technology of China, Hefei, People's Republic of China*
[7]*Universidad de los Andes, Bogotá, Colombia*
[8]*Faculty of Mathematics and Physics, Center for Particle Physics, Charles University, Prague, Czech Republic*
[9]*Czech Technical University in Prague, Prague, Czech Republic*
[10]*Center for Particle Physics, Institute of Physics, Academy of Sciences of the Czech Republic, Prague, Czech Republic*
[11]*Universidad San Francisco de Quito, Quito, Ecuador*
[12]*LPC, Université Blaise Pascal, CNRS/IN2P3, Clermont, France*
[13]*LPSC, Université Joseph Fourier Grenoble 1, CNRS/IN2P3, Institut National Polytechnique de Grenoble, Grenoble, France*
[14]*CPPM, Aix-Marseille Université, CNRS/IN2P3, Marseille, France*
[15]*LAL, Université Paris-Sud, CNRS/IN2P3, Orsay, France*
[16]*LPNHE, Universités Paris VI and VII, CNRS/IN2P3, Paris, France*
[17]*CEA, Irfu, SPP, Saclay, France*
[18]*IPHC, Université de Strasbourg, CNRS/IN2P3, Strasbourg, France*
[19]*IPNL, Université Lyon 1, CNRS/IN2P3, Villeurbanne, France and Université de Lyon, Lyon, France*
[20]*III. Physikalisches Institut A, RWTH Aachen University, Aachen, Germany*
[21]*Physikalisches Institut, Universität Freiburg, Freiburg, Germany*
[22]*II. Physikalisches Institut, Georg-August-Universität Göttingen, Göttingen, Germany*
[23]*Institut für Physik, Universität Mainz, Mainz, Germany*
[24]*Ludwig-Maximilians-Universität München, München, Germany*
[25]*Fachbereich Physik, Bergische Universität Wuppertal, Wuppertal, Germany*
[26]*Panjab University, Chandigarh, India*
[27]*Delhi University, Delhi, India*
[28]*Tata Institute of Fundamental Research, Mumbai, India*
[29]*University College Dublin, Dublin, Ireland*
[30]*Korea Detector Laboratory, Korea University, Seoul, Korea*
[31]*CINVESTAV, Mexico City, Mexico*
[32]*Nikhef, Science Park, Amsterdam, The Netherlands*
[33]*Radboud University Nijmegen, Nijmegen, The Netherlands and Nikhef, Science Park, Amsterdam, The Netherlands*
[34]*Joint Institute for Nuclear Research, Dubna, Russia*
[35]*Institute for Theoretical and Experimental Physics, Moscow, Russia*
[36]*Moscow State University, Moscow, Russia*
[37]*Institute for High Energy Physics, Protvino, Russia*
[38]*Petersburg Nuclear Physics Institute, St. Petersburg, Russia*
[39]*Institució Catalana de Recerca i Estudis Avançats (ICREA) and Institut de Física d'Altes Energies (IFAE), Barcelona, Spain*
[40]*Stockholm University, Stockholm and Uppsala University, Uppsala, Sweden*
[41]*Lancaster University, Lancaster LA1 4YB, United Kingdom*
[42]*Imperial College London, London SW7 2AZ, United Kingdom*
[43]*The University of Manchester, Manchester M13 9PL, United Kingdom*
[44]*University of Arizona, Tucson, Arizona 85721, USA*
[45]*University of California Riverside, Riverside, California 92521, USA*
[46]*Florida State University, Tallahassee, Florida 32306, USA*
[47]*Fermi National Accelerator Laboratory, Batavia, Illinois 60510, USA*
[48]*University of Illinois at Chicago, Chicago, Illinois 60607, USA*
[49]*Northern Illinois University, DeKalb, Illinois 60115, USA*
[50]*Northwestern University, Evanston, Illinois 60208, USA*
[51]*Indiana University, Bloomington, Indiana 47405, USA*

^{52}*Purdue University Calumet, Hammond, Indiana 46323, USA*
^{53}*University of Notre Dame, Notre Dame, Indiana 46556, USA*
^{54}*Iowa State University, Ames, Iowa 50011, USA*
^{55}*University of Kansas, Lawrence, Kansas 66045, USA*
^{56}*Kansas State University, Manhattan, Kansas 66506, USA*
^{57}*Louisiana Tech University, Ruston, Louisiana 71272, USA*
^{58}*Boston University, Boston, Massachusetts 02215, USA*
^{59}*Northeastern University, Boston, Massachusetts 02115, USA*
^{60}*University of Michigan, Ann Arbor, Michigan 48109, USA*
^{61}*Michigan State University, East Lansing, Michigan 48824, USA*
^{62}*University of Mississippi, University, Mississippi 38677, USA*
^{63}*University of Nebraska, Lincoln, Nebraska 68588, USA*
^{64}*Rutgers University, Piscataway, New Jersey 08855, USA*
^{65}*Princeton University, Princeton, New Jersey 08544, USA*
^{66}*State University of New York, Buffalo, New York 14260, USA*
^{67}*Columbia University, New York, New York 10027, USA*
^{68}*University of Rochester, Rochester, New York 14627, USA*
^{69}*State University of New York, Stony Brook, New York 11794, USA*
^{70}*Brookhaven National Laboratory, Upton, New York 11973, USA*
^{71}*Langston University, Langston, Oklahoma 73050, USA*
^{72}*University of Oklahoma, Norman, Oklahoma 73019, USA*
^{73}*Oklahoma State University, Stillwater, Oklahoma 74078, USA*
^{74}*Brown University, Providence, Rhode Island 02912, USA*
^{75}*University of Texas, Arlington, Texas 76019, USA*
^{76}*Southern Methodist University, Dallas, Texas 75275, USA*
^{77}*Rice University, Houston, Texas 77005, USA*
^{78}*University of Virginia, Charlottesville, Virginia 22901, USA*
^{79}*University of Washington, Seattle, Washington 98195, USA*

We present a search for Kaluza-Klein (KK) particles predicted by models with universal extra dimensions (UED) using a data set corresponding to an integrated luminosity of 7.3 fb^{-1}, collected by the D0 detector at a $p\bar{p}$ center-of-mass energy of 1.96 TeV. The decay chain of KK particles can lead to a final state with two muons of the same charge. This signature is used to set a lower limit on the compactification scale of $R^{-1} > 260$ GeV in a minimal UED model.

The existence of extra dimensions in addition to the $3 + 1$ dimensions of space-time has been postulated as a possible solution to the problem of the large hierarchy of scales in the standard model (SM). In models with universal extra dimensions (UED), all particles propagate in the extra dimensions [1]. In this Letter, we study a minimal UED (mUED) model, which has only one extra dimension [2].

Each SM particle in the mUED model is associated with a set of excited Kaluza-Klein (KK) states when viewed in $3 + 1$ dimensions. Since compactification of the extra dimensions leads to periodic boundary conditions, the KK states have discrete masses of the order of R^{-1}, where R is the radius of the compact dimension. If one-loop corrections are applied, the mass spectrum of the KK modes also depends on a cutoff scale for boundary terms, which is chosen to be 10 TeV [2]. Gluon KK modes (g_1) are the heaviest particles, followed by quarks [SU(2) doublet Q_1 or singlet q_1], gauge bosons (Z_1/W_1), leptons [SU(2) doublet L_1 or singlet ℓ_1], and the KK photon (γ_1), which is the lightest KK particle (LKP) and does not decay. The LKP is also a dark matter candidate [3].

Previous searches for KK particles predicted by a modified UED model have been conducted by the D0 [4] Collaboration at the Fermilab Tevatron Collider and by the ATLAS [5] Collaboration at the CERN LHC in diphoton final states. In this model, gravity mediation allows decays of the LKP into a photon plus a light KK graviton. A search for events with two leptons of the same charge, which can be interpreted in a mUED model, has been performed by ATLAS [6], but no dedicated study of the mUED model has so far been performed at a collider. Constraints from precision electroweak data [1], from the measurements of the muon anomalous magnetic moment and of the $b \rightarrow s\gamma$ branching ratio [7], indicate that the scale R^{-1} can be as low as ≈ 300 GeV, making KK particles accessible at the Tevatron. In this Letter, the first search for mUED in the final state with two leptons of the same charge is presented using data corresponding to 7.3 fb^{-1} of integrated luminosity collected by the D0 detector [8] at $\sqrt{s} = 1.96$ TeV.

At the Tevatron, KK gluons or quarks are mainly produced in pairs, as shown in Fig. 1. In the subsequent
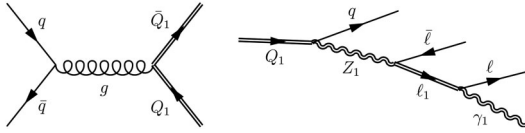
FIG. 1. (a) Production of a pair of KK quarks ($Q_1 \bar{Q}_1$).
(b) Decay of a KK quark into a jet, two oppositely charged
leptons, and the LKP. Double lines indicate KK excitations. A
similar cascade decay occurs for the second KK quark, leading
to several leptons of the same charge in the final state.

TABLE I. Masses of KK particles for each R^{-1} value used in
the MC generation with corresponding total production cross
section.

R^{-1} (GeV)	Masses (GeV)					Cross Section (pb)
	γ_1	Z_1	g_1	ℓ_1	Q_1	
200	201	230	269	207	249	34.9 ± 0.2
215	216	245	287	222	266	20.4 ± 0.1
230	231	260	305	238	283	12.1 ± 0.1
245	246	274	323	253	300	7.24 ± 0.05
260	261	289	341	268	317	4.39 ± 0.03
275	276	304	359	284	334	2.69 ± 0.02
290	291	319	377	299	351	1.65 ± 0.01
305	306	335	395	314	368	1.02 ± 0.06
320	321	350	413	330	385	0.63 ± 0.01

cascade decay, up to four charged leptons are produced.
Since the masses of the extra particles predicted by the
mUED models are nearly degenerate, the leptons are emit-
ted with low transverse momentum and might escape
detection. In this analysis, we select events with two muons
of the same charge.

The D0 detector [8] consists of tracking systems and
calorimeters. The innermost part is a tracking system
where charged particles are detected by the silicon micro-
strip and central fiber tracking detectors, located within a
2 T solenoid. The tracking system is surrounded by a
liquid-argon and uranium sampling calorimeter. Particle
energies are measured in the electromagnetic and hadronic
calorimeters within a pseudorapidity range of $|\eta| < 4.2$
[9]. Jets are reconstructed with a cone algorithm using a
radius of $\mathcal{R} = 0.5$ [10] in the calorimeter. The central and
forward muon detectors are composed of a layer of wire
chambers and scintillators in front of a 1.8 T toroid magnet
and two layers outside the toroid. Missing transverse
energy is measured from the vector sum of the calorimeter
cell energies in the xy plane [11]. A correction for the
energy response of muons, electrons, and jets is applied.

The backgrounds from Z + jets, W + jets, and $t\bar{t}$ pro-
duction are modeled by the ALPGEN [12] Monte Carlo
(MC) event generator, interfaced with PYTHIA [13] for
showering and hadronization. Diboson production (WW,
WZ, and ZZ) is simulated by PYTHIA. The CTEQ6L1
parametrization of the parton distribution functions
(PDFs) is used [14]. Higher-order cross sections for dibo-
son and W/Z + jets production are calculated by MCFM
[15], and the cross section of $t\bar{t}$ pair production is taken
from [16]. The dominant source of background is pairs of
muons with the same charge from heavy flavor jets. This
background contribution is estimated from data and is
described in detail in the following.

Signal MC events are generated for 9 different values of
R^{-1}, covering the range from 200 to 320 GeV in steps of
15 GeV, using PYTHIA with the CTEQ5L PDF parametri-
zation [17]. The production cross sections and masses of
KK particles are taken from PYTHIA. They are given in
Table I for each R^{-1} and with all KK gluon and quark
production modes included. All decay mechanisms leading
to like-charge dimuon final states are taken into account.
The decay branching fractions for all KK particles are
given by the mUED model. After simulating all cascade

decays, approximately 1% of events have two like-charged
muons.

All signal and background MC events pass through the
full GEANT-based simulation of the detector [18] and are
reconstructed using the same algorithms as used for data.
To simulate detector noise and multiple $p\bar{p}$ interactions,
MC events are overlaid with data events from random
beam crossings.

Events are selected by requiring that they pass at least
one single muon trigger condition. We require that each
event must contain at least two muons of the same charge.
The track in the muon system must be matched to a track in
the central tracking system with detector $|\eta| < 1.5$. We
reject cosmic rays by requiring the associated scintillator
hits in the muon system to be consistent with originating
from a $p\bar{p}$ collision, the distance of closest approach of the
muon tracks to the $p\bar{p}$ interaction vertex to be less than
0.05 cm, and the differences between the z coordinates of
the distance of closest approach of each muon and the $p\bar{p}$
interaction vertex to be <1 cm. We require $\Delta\phi_{\mu\mu} <$
2.9 rad for the azimuthal angle between the two muons
in order to reject multijet background in which there are
back-to-back jets which can contain muons from semi-
leptonic meson decay and $\Delta\phi_{\mu\mu} > 0.25$ rad to reject
muons originating from the same jet. The transverse
momenta of the leading and next-to-leading muons have
to be $15 < p_{T_1} < 200$ GeV and $p_{T_2} > 10$ GeV, respec-
tively. The invariant mass of the muon pair must be in
the range $M_{\mu\mu} < 250$ GeV. The upper limits on the muon
p_T and dimuon invariant mass reduce the number of events
with one of the muon charges misreconstructed. In addi-
tion, we reject events with $\not{E}_T < 25$ GeV, since multijet
background dominates at low $\not{E}_T$.

To discriminate between isolated muons from signal and
muons contained in jets, we define the isolation in the
calorimeter, I^{cal}, as the sum of the energy deposited in
the calorimeter within an annulus of $0.1 < \mathcal{R} < 0.4$, di-
vided by the muon p_T, and the isolation in the tracking

detector, I^{trk}, as the sum of the p_T of all charged particles within a cone of $\mathcal{R} = 0.5$ around the muon, excluding the muon itself, divided by p_T^μ. At least one of the two muons is required to be isolated with $I^{\mathrm{cal}} < 0.4$ and $I^{\mathrm{trk}} < 0.12$.

We estimate the multijet background by defining a signal- and a background-enriched sample. The signal-enriched sample comprises events where the requirement on the isolation of the second muon in the tracking detector is relaxed to $I^{\mathrm{trk}} < 0.25$. To define a background-enriched sample, we require that the second muon fails the isolation requirement. A normalization factor is calculated for each jet multiplicity, given by the ratio of the number of events in the signal- and background-enriched samples in a multijet-dominated region where the p_T of the most isolated muon is $5 < p_T < 10$ GeV. The multijet background is determined by multiplying the background-enriched sample with this normalization factor in the region where the p_T of the most isolated muon is >10 GeV.

In the high p_T region, there is a significant contribution to the background-enriched sample from SM processes other than multijet, particularly from $W +$ jets production, with an isolated muon from the W boson decay and a nonisolated muon embedded in the jet. This SM background is modeled by applying the selection used to define the background-enriched sample to MC events. The resulting SM background distributions, corrected with the same normalization factors as used for data, are subtracted from the corrected distribution of the background-enriched data sample to obtain an estimate of the multijet background.

Events from $Z \to \mu\mu$ decays enter our sample mainly through misreconstruction of one of the muon charges. This background is estimated from simulation. We use data to determine the corresponding systematic uncertainty by comparing the two independent charge measurements in the central tracking detector and the muon detector [19]. We determine the rate of muons with an incorrectly measured charge by counting the number of events where the two measurements disagree. The number of charge-flip events in data is in good agreement with the number of like-charged $Z \to \mu\mu$ events predicted by the simulation.

To improve the discrimination between signal and background, a boosted decision tree (BDT) [20] is trained using p_{T_1}, p_{T_2}, $M_{\mu\mu}$, $\Delta\phi_{\mu\mu}$, and the number of jets as input variables. Further input variables are the χ^2 of the fit of the muon tracks to reject badly reconstructed muons, the transverse masses $M_T = \sqrt{2\not{E}_T p_T [1 - \cos\Delta\phi(\vec{\not{E}}_T, \mu)]}$ calculated separately for each muon, and the scalar product of $\not{E}_T$ and p_{T_2}. This rejects multijet background events with small $\not{E}_T$ or p_{T_2}.

The distributions of $\not{E}_T$ and p_{T_1} for data and background are shown in Fig. 2, together with signal for $R^{-1} = 260$ GeV. The BDT is trained separately for each signal point with different R^{-1}. The BDT output distribution is shown in Fig. 3, and the event yields in the data are compared to the expected number of background and
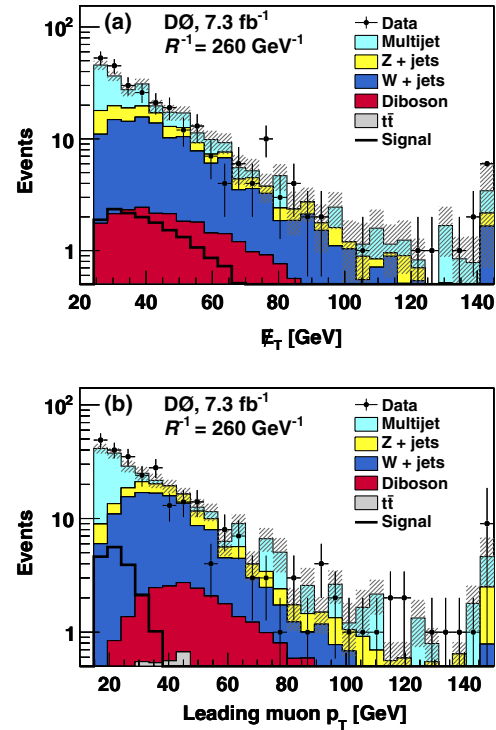

FIG. 2 (color online). Distribution of (a) $\not{E}_T$ and (b) p_{T_1} for data and background, compared to a signal with $R^{-1} = 260$ GeV. The shaded band shows the statistical uncertainty on the background estimation. All entries exceeding the range of the histogram are added to the last bin.

signal events in Table II. Signal is concentrated in the region where the BDT output is >0.

Systematic uncertainties on the normalization of both background and signal, including their correlations, are taken into account. These include theoretical uncertainties on SM background cross sections (7–15%) and the uncertainties on the rate of multijet background (40%), signal efficiency from choice of PDF parametrization (4%), integrated luminosity (6.1%), jet energy scale (4%), rate of
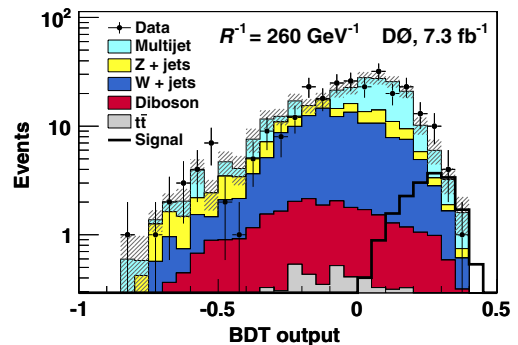

FIG. 3 (color online). Distribution of the BDT output for data and background, compared to a signal with $R^{-1} = 260$ GeV. The shaded band shows the statistical uncertainty on the background estimation.

TABLE II. Expected number of events for backgrounds, event yields in data, and expected number of events for a signal with $R^{-1} = 260$ GeV after the final selection and requiring a BDT output >0 (for illustrative purposes, this cut is not used for limit estimation). The total uncertainties are also given.

Process	Final Selection	BDT output >0
Diboson	21 ± 3	6 ± 1
Z + jets	39 ± 9	13 ± 3
W + jets	109 ± 14	38 ± 5
$t\bar{t}$	6 ± 1	2 ± 1
Multijet	95 ± 41	63 ± 27
Total Background	271 ± 45	123 ± 28
Data	273	126
Signal	18 ± 1	18 ± 1

Z/γ^* production with an incorrectly reconstructed muon charge (21%), trigger efficiency (6%), and muon reconstruction and isolation (2%).

The entire differential distribution of the BDT output is used to set limits on the product of the cross section and the branching ratio with the CL_s method [21] and a profiling technique to reduce the impact of systematic uncertainties [22]. Observed and median expected upper limits at 95% C.L. on the product of the cross section σ and the branching fraction $\mathcal{B}$ into like-charged muon pairs are shown in Fig. 4 as a function of R^{-1}. The theoretical cross section of the mUED model intersects the expected limit at $R^{-1} = 275$ GeV and the observed at $R^{-1} = 260$ GeV, which corresponds to a mass of 317 GeV of the lightest KK quark in the mUED model.

In summary, we present a search for extra dimensions in the mUED model using 7.3 fb^{-1} of integrated luminosity collected by the D0 experiment. The first direct lower limit on the compactification scale of the extra dimension in the mUED model is set as $R^{-1} = 260$ GeV.
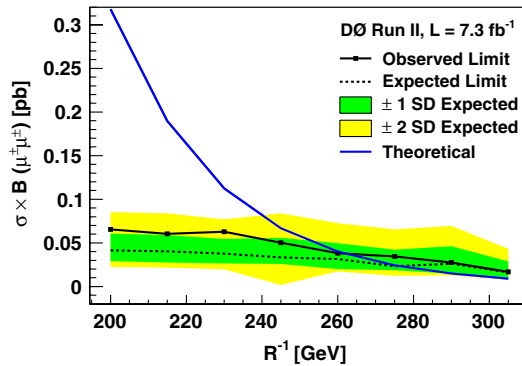

FIG. 4 (color online). Observed and median expected 95% C.L. limits on $\sigma\mathcal{B}(\mu^\pm\mu^\pm)$ as a function of R^{-1} compared to $\sigma\mathcal{B}(\mu^\pm\mu^\pm)$ calculated with the mUED model. The bands represent ± 1 and ± 2 standard deviations (SD) around the median expected limits.

*Deceased.
†Visitor from Augustana College, Sioux Falls, SD, USA.
‡Visitor from The University of Liverpool, Liverpool, UK.
§Visitor from UPIITA-IPN, Mexico City, Mexico.
‖Visitor from DESY, Hamburg, Germany.
¶Visitor from SLAC, Menlo Park, CA, USA.
**Visitor from University College London, London, UK.
††Visitor from Centro de Investigacion en Computacion—IPN, Mexico City, Mexico.
‡‡Visitor from ECFM, Universidad Autonoma de Sinaloa, Culiacán, Mexico.
§§Visitor from Universität Bern, Bern, Switzerland.

[1] T. Appelquist, H.-C. Cheng, and B. A. Dobrescu, Phys. Rev. D **64**, 035002 (2001).
[2] H.-C. Cheng, K. T. Matchev, and M. Schmaltz, Phys. Rev. D **66**, 056006 (2002).
[3] H.-C. Cheng, J. L. Feng, and K. T. Matchev, Phys. Rev. Lett. **89**, 211301 (2002).
[4] V. M. Abazov *et al.* (D0 Collaboration), Phys. Rev. Lett. **105**, 221802 (2010).
[5] G. Aad *et al.* (ATLAS Collaboration), Eur. Phys. J. C **71**, 1744 (2011).
[6] G. Aad *et al.* (ATLAS Collaboration), J. High Energy Phys. 10 (2011) 107.
[7] K. Agashe, N. G. Deshpande, and G. H. Wu, Phys. Lett. B **514**, 309 (2001); T. Appelquist and B. A. Dobrescu, *ibid.* **516**, 85 (2001).
[8] V. M. Abazov *et al.* (D0 Collaboration), Nucl. Instrum. Methods Phys. Res., Sect. A **565**, 463 (2006).
[9] The D0 detector coordinate system is right-handed, with the z axis pointing in the proton beam direction. The y axis points upward, and the azimuthal angle ϕ is measured from the x axis. Pseudorapidity is defined as $\eta = -\ln[\tan(\theta/2)]$, where θ is the polar angle.
[10] G. C. Blazey *et al.*, arXiv:hep-ex/0005012.
[11] Missing transverse energy is defined as $\vec{\cancel{E}}_T = -\sum_i (E^i_{T,x}, E^i_{T,y})$, where $E^i_{T,x} = E^i \sin\theta^i \cos\phi^i$ and $E^i_{T,y} = E^i \sin\theta^i \sin\phi^i$. Here, E^i is the energy deposited in the ith calorimeter cell and the angles θ^i and ϕ^i define the direction from the origin of the coordinate system to the ith calorimeter cell. We also define $\cancel{E} \equiv |\vec{\cancel{E}}_T|$.
[12] M. L. Mangano, F. Piccinini, A. D. Polosa, M. Moretti, and R. Pittau, J. High Energy Phys. 07 (2003) 001. We use version 2.05.

[13] T. Sjöstrand, S. Mrenna, and P. Skands, J. High Energy Phys. 05 (2006) 026. We use version 6.421 for generating the signal MC events.

[14] J. Pumplin, D. R. Stump, J. Huston, H.-L. Lai, P. Nadolsky, and W.-K. Tung, J. High Energy Phys. 07 (2002) 012; D. Stump, J. Huston, J. Pumplin, W.-K. Tung, H.-L. Lai, S. Kuhlmann, and J. F. Owens, *ibid.* 10 (2003) 046.

[15] J. Campbell and R. K. Ellis, Phys. Rev. D **65**, 113007 (2002); J. Campbell, R. K. Ellis, and D. Rainwater, *ibid.* **68**, 094021 (2003).

[16] S. Moch and P. Uwer, Phys. Rev. D **78**, 034003 (2008).

[17] H. L. Lai, J. Huston, S. Kuhlmann, J. Morfin, F. Olness, J. F. Owens, J. Pumplin, and W. K. Tung (CTEQ Collaboration), Eur. Phys. J. C **12**, 375 (2000).

[18] R. Brun, F. Carminati, and S. Giani, CERN Report No. CERN-W5013, 1993.

[19] V. M. Abazov *et al.* (D0 Collaboration), Phys. Rev. D **84**, 092002 (2011).

[20] A. Hoecker *et al.*, Proc. Sci., ACAT (2007) 040.

[21] T. Junk, Nucl. Instrum. Methods Phys. Res., Sect. A **434**, 435 (1999); A. Read, J. Phys. G **28**, 2693 (2002).

[22] W. Fisher, FERMILAB Report No. FERMILAB-TM-2386-E, 2006.